



*J. Serb. Chem. Soc.* 77 (12) 1775–1785 (2012)  
JSCS–4388

## Effect of cooling rate on the microstructure and porosity of alumina produced by freeze casting

JESÚS M. RODRÍGUEZ-PARRA, RODRIGO MORENO\* and MARÍA ISABEL NIETO

*Institute of Ceramics and Glass, CSIC, Kelsen 5, 28049 Madrid, Spain*

(Received 18 November, revised 3 December 2012)

**Abstract:** Freeze casting is a well-known shaping technique for the production of materials with directional porosity. One of the major problems is the difficulty to control the cooling rate, thus leading to gradients in pore size and homogeneity. This work deals with the manufacture of alumina ceramics with directional porosity by freeze casting of aqueous suspensions. An experimental set-up was prepared in order to apply different cooling rates. Freeze casting tests were performed with an aqueous alumina suspension after optimization of its rheological behavior. The porosity and microstructural features of the sintered bodies produced under different experimental conditions were studied and analyzed. It was concluded that the cooling rate influences the microstructure while the final temperature has a much lower influence. In addition, microstructural analysis showed that there was a gradient in the directionality of the pores, being lower at the bottom and the top and higher in the central region of the specimens.

**Keywords:** suspensions; shaping; ceramics; porous materials; alumina; microstructures.

### INTRODUCTION

The design of materials with tailored porosity has received increasing attention in the field of porous ceramics, due to the large number of their applications in different technologies.<sup>1–5</sup> Within the available techniques for the manufacture of porous materials, great effort has been devoted to the study of the application of freeze-casting to obtain ceramics with aligned porosity,<sup>6–13</sup> and to establish the influence of different processing variables on the pore size and distribution.

The freeze casting process is based on the fast freezing of a suspension inside a non-porous mould and the subsequent elimination of liquid by sublimation under vacuum conditions. Different liquids have been employed, such as water and camphene,<sup>14,15</sup> which require different freezing temperatures. The obtained

\* Corresponding author. E-mail: rmoreno@icv.csic.es  
doi: 10.2298/JSC121018132R

porosity is a replica of the frozen liquid; hence, the solid content of the suspensions is directly related to the porosity volumes allowed. When aqueous suspensions are used, it was demonstrated that the presence of a binder is mandatory. Otherwise, the frozen structure formed collapses during sublimation and the pores tend to close.<sup>8</sup>

The most important parameters involved in the process are the freezing temperature, the rate and manner of cooling and the solids content.<sup>6–9,16–23</sup> Cooling temperatures ranging from  $-20/-80$  °C down to liquid nitrogen temperature ( $-196$  °C) are normally used. The solids content determines the volume of the porosity and the pore size.<sup>6,7,9,21,22</sup> There is an optimal range of suspension concentrations required to obtain a handling solid and to avoid microstructure collapse if the solid content is very high.

The parameter that dominantly influences the orientation of the porosity is the cooling procedure.<sup>16–19</sup> Bulk freezing leads to porous materials with a homogeneous distribution of porosities, while it is possible to obtain microstructures with directionally aligned porosities if only the bottom part of suspension is in contact with the freezing agent, so the ice grows in a vertical direction and aligned channels will be obtained after the sublimation process. The cooling process can be performed at a constant temperature or constant cooling rate. When the temperature is maintained constant, the microstructure shows the formation of different oriented colonies with aligned pores, while if the freezing is performed at a constant rate, a porous structure with unidirectional channels is obtained.<sup>8</sup> The size of the ice dendrites is a function of the formation velocity of the ice front;<sup>9</sup> consequently, the rate of freezing determines the size of obtained pores.<sup>16–19</sup>

Poly(vinyl alcohol) (PVA) and glycerol are the most frequently used additives for freezing.<sup>10–12,17,19,24–26</sup> PVA is usually added in concentrations ranging from 2 to 20 wt. %, and it was observed that the dendrites and consequently the pores are finer as the PVA content increases.<sup>12,24</sup> The addition of PVA also transforms the non-interconnected lamellar pores into small and interconnected lamellar pores.<sup>24</sup> Glycerol reduces the volumetric expansion of water and binds to water molecules, reducing the size of the growing ice crystals.<sup>9,25,26</sup> The concentration of glycerol is always related to water, and it is normally added in the range from 10 to 30 wt. %.

In the present work, porous alumina bodies with aligned porosities were shaped by directionally freeze drying at a constant rate of cooling. The influence of freezing rate and freezing temperature on the porosity and microstructure of the sintered alumina specimens was studied and discussed.

#### EXPERIMENTAL

Commercial  $\alpha$ -alumina (Ceralox, Condea HPA05, USA), with an average particle size of  $0.4 \mu\text{m}$  and a specific surface area of  $9.5 \text{ m}^2 \text{ g}^{-1}$  was used. The colloidal stability was studied and reported in a previous work, in which the isoelectric point was reported to occur at pH 9

and the effect of polyelectrolyte (an ammonium salt of poly(acrylic acid) (PAA, Duramax D3005, Rohm & Haas, PA, USA) was also studied.<sup>27</sup> This deflocculant is supplied as an aqueous solution with a concentration of 35 wt. % of active matter and has a pH 7–8 and a density of 1.16 g cm<sup>-3</sup>. The maximum stability was achieved at a concentration of PAA of 0.8 wt. % (*i.e.*, 0.35 wt. % active matter) on a dry solids basis.

Commercial glycerol (Sigma-Aldrich, Germany) was used as a cryoprotector. Concentrated suspensions were prepared to a solids loading of 35 vol. % (*i.e.*, 67 wt. %) by adding 20 wt. % of glycerol (with regard to solids). According to previous studies, these conditions led to good properties in terms of pores volume and size.<sup>19</sup> The suspensions were homogenized during ball milling for 6 h.

The rheological behavior of fresh ball milled suspensions was studied with a rheometer (RS50, Haake, Germany) using a double-cone/plate sensor configuration (DC60/2°, Haake, Germany). The tests were performed under controlled rate (CR) conditions using a three stage program with a linear increase of shear rate from 0 to 1000 s<sup>-1</sup> in 300 s, a plateau at 1000 s<sup>-1</sup> for 120 s, and a further decrease to zero shear rate in 300 s. The flow curves of the optimized suspension were measured as a function of ageing time, until 9 days after preparation. The particle size was measured using laser diffraction equipment (Mastersizer S, Malvern, UK) on suspensions diluted to 0.01 g dm<sup>-3</sup>.

A 22 cm in height copper cylinder was designed as a support for the mould. This mould consisted of a metallic piece on the bottom and plastic walls, in order to allow the transmission of heat from the bottom to the top of the suspension when the copper cylinder was immersed in liquid N<sub>2</sub>. A glass fiber matt was used as an isolating component to allow proper control of the cooling rate. Two different devices were used to contain the liquid nitrogen. Firstly, a simple metal container with isolating fibers and polyethylene rings was designed in order to minimize nitrogen loss. Furthermore, the liquid nitrogen was poured in a Dewar vessel supported on a metal box so that the height of the support and hence the cooling rate of the suspension container could be controlled. Temperature control was realized between –200 and 200 °C using a thermocouple (Type T, Watlow No: OKT30B12B, UK) connected to a power source (ITC 503s, Oxford Instruments, UK) where the temperature was revealed. Considering the foreseen cooling procedures (rates), freeze cast samples were dried using a freeze dryer (CRYODOS-50, Telstar, Terrassa, Spain) for 24 h. The condenser temperature was 50 °C and the conditions of the storage camera were 20 °C and 50 Pa. Further characterization was performed for samples prepared at –60 and –90 °C using the Dewar, and at –60 °C in the metallic container. These samples were labeled as –60D, –90D and –60C, respectively.

The green density of freeze cast specimens was measured by the Archimedes method using mercury. The green specimens were sintered at 1500 °C for 2 h in an electric furnace. The sintered specimens were characterized by microstructure observations using a field emission scanning electron microscopy (FE–SEM, Hitachi S-4700 type I). The porosity was measured by mercury intrusion porosimetry (Poremaster, Quantachrome Corp., USA).

## RESULTS AND DISCUSSION

The stability of optimized alumina suspensions (with deflocculant and glycerol) was studied by measuring the flow curves daily until the viscosity started to increase. The flow curves of the fresh suspension and after different ageing times are shown in Fig. 1. The suspensions had a low viscosity until day 7 and were nearly Newtonian. The evolution of the viscosity with time is shown in Fig.

2, from which it can be seen that the viscosity first remained constant and then sharply increased after 9 days.

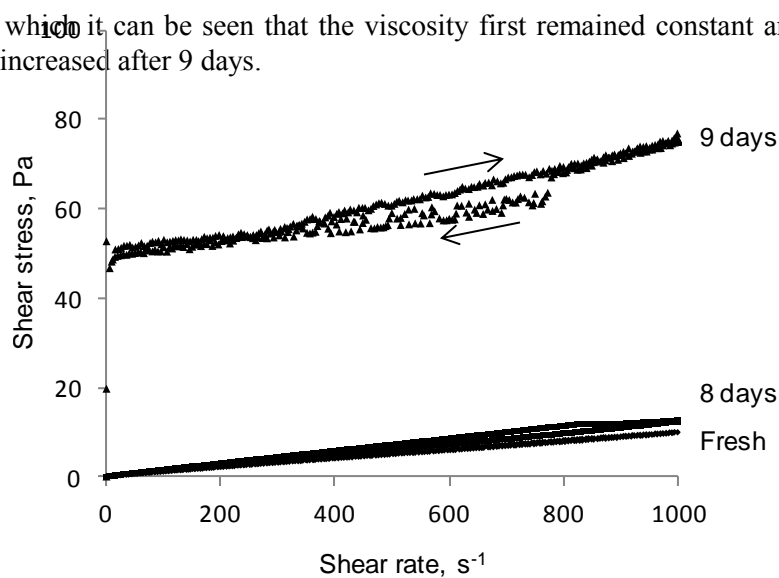


Figure 1. Flow curves of alumina suspensions, just after prepared and after 8 and 9 days ageing.

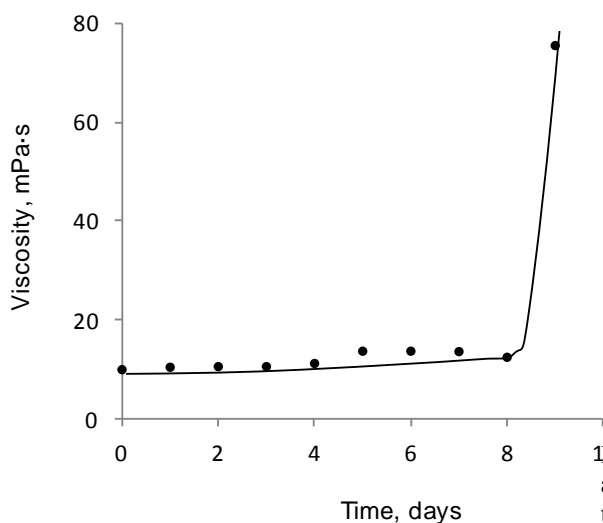


Figure 2. Evolution of viscosity of alumina suspension with ageing time (shear rate,  $1000 \text{ s}^{-1}$ ).

Particle size distribution was measured after dilution of the concentrated suspensions used for the rheological behavior studies. The distribution curve was bimodal with a major contribution of fine particles centered on less than  $1 \mu\text{m}$  with a smaller fraction of the particles having sizes less than  $10 \mu\text{m}$ . There was no change in the size distribution during ageing for a few days, but the coarse fraction seems to increase after that, in agreement with the rheological behavior.

The particle size distributions of fresh suspensions and after 9 days of ageing are shown in Fig. 3.

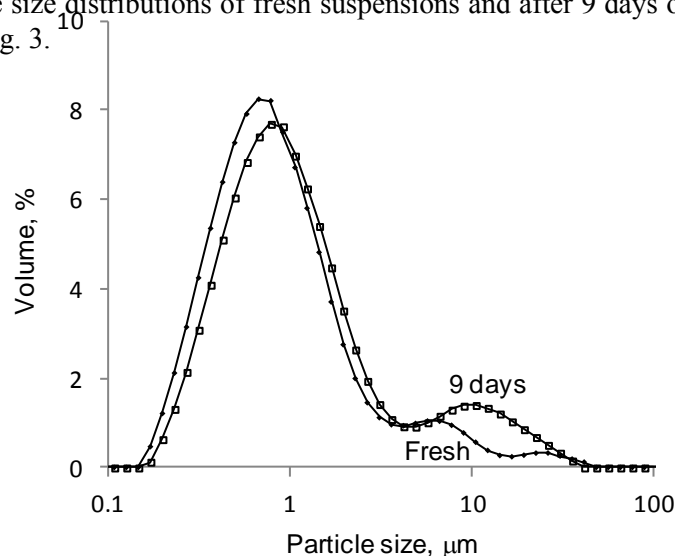


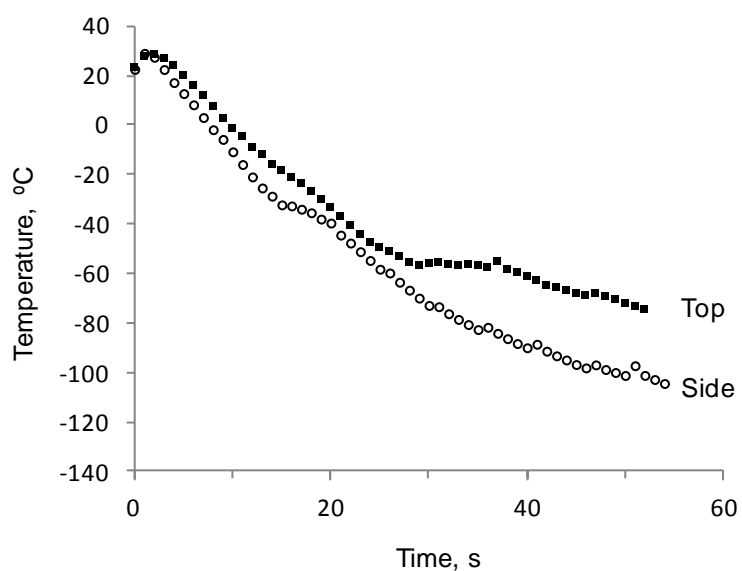
Figure 3. Particle size distribution as measured for the fresh suspension and after 9 days ageing.

Once the stability of the suspensions was ensured, the freezing device was optimized in order to allow for the control of the cooling temperature. Thus, the thermocouple was calibrated by measuring the voltage as a function of temperature in the range from  $-4.19$  to  $0.273$  mV.

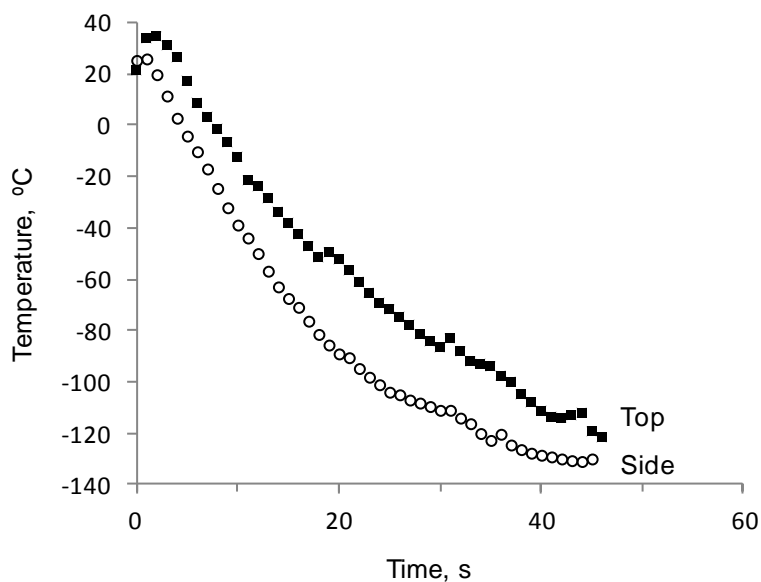
The variations of the temperature with time for the two types of cooling devices described in the experimental section, *i.e.*, the Dewar, and the simple metal container, are shown in Fig. 4. In both cases, the temperature was measured at the top of the metal container, in contact with the suspension, and in the lateral surface of the copper cylinder. It can be seen that the use of a Dewar assured a more homogeneous temperature variation with higher cooling rates and that a lower temperature was reached, as expected. By fitting the curves in the linear range (to  $-60$  °C), calculated rates were  $6.8$  and  $3.4$  °C  $\text{min}^{-1}$  for the Dewar and the metal container, respectively. With this control of temperature, the samples were frozen and dried as described above, giving the samples  $-60\text{D}$ ,  $-90\text{D}$  and  $-60\text{C}$  were obtained. The green bodies obtained after freeze-drying for 48 h had densities of  $1.63 \pm 0.02$  g  $\text{cm}^{-3}$  (*i.e.*, 41 % of theoretical density). These samples were sintered at  $1500$  °C with a 2-h soaking time.

The data obtained by Hg-porosimetry for the sintered bodies are given in Table I. All samples exhibited macroporosity, which was slightly higher for the samples obtained in the metal container, due to the slower cooling rate. According to Table I, it appears that the cooling rate had no significant effect on the total

pore volume. However, samples cooled in the Dewar had a narrower pore size distribution (Fig. 5), confirming their higher homogeneity.



(a)



(b)

Figure 4. Variation of temperature with time when cooling with the simple metal container (a), and the Dewar (b). Temperature is measured in both cases at the top of the metal container, in contact with the suspension, and in the lateral surface of the copper cylinder.

Table 1. Density and porosity of the samples obtained at different cooling conditions

Sample	$\rho_{\text{green}}$ g cm <sup>-3</sup>	$\rho_{\text{sintered}}$ g cm <sup>-3</sup>	Pore volume cm <sup>3</sup> g <sup>-1</sup>	Pore diameter $\mu\text{m}$	Pore area m <sup>2</sup> g <sup>-1</sup>
-60C	1.63	2.31	0.17	4.6	0.14
-60D	1.63	2.36	0.15	4.8	0.17
-90D	1.65	2.48	0.15	4.6	0.13

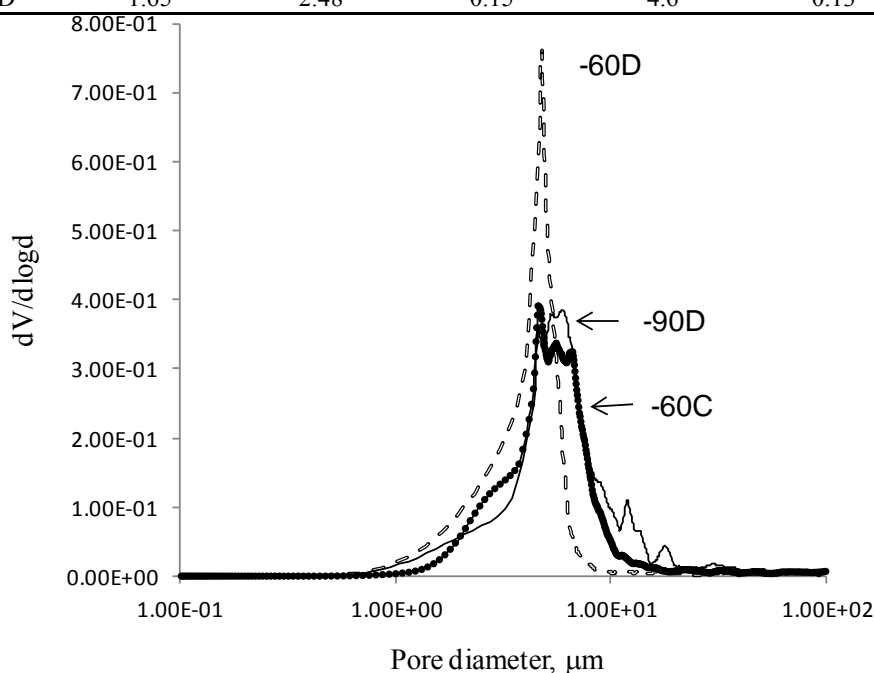


Figure 5. Pore size distribution of sintered alumina samples prepared at the different cooling conditions.

In spite of the similarities in the macroporous structure, SEM observations demonstrated that there were some differences among the variously prepared samples. Low magnification SEM pictures of the three studied samples are shown in Fig. 6. Directional porosity is clear in all samples, but the sample -60D is more homogeneous than -60C, which exhibited lower microstructural uniformity since the areas with directional porosity and dense areas were combined.

SEM observations at higher magnification, Fig. 7, were performed in order to compare the microstructural features of samples prepared under different conditions. Sample -60C revealed a lower degree of directionality and the pores were larger in diameter than those in the other two samples both having rather similar pore sizes and size distributions, which is in good agreement with porosimetry results. Comparing all these microstructures, it was noticed that the cell walls were larger for the sample -60C. This sample, obtained with the lowest cooling rate, revealed characteristics in agreement with results of Deville *et*

*al.*<sup>8,18</sup> who reported that both the size of the pores and the cell walls were larger if the cooling rate was lower.

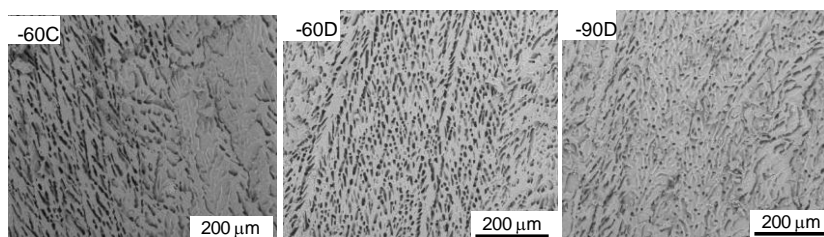


Figure 6. General view of the microstructure of the sintered alumina samples prepared at the different cooling conditions.

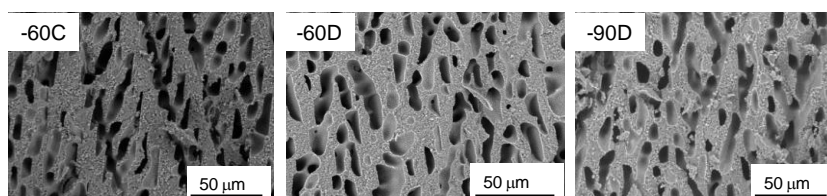


Figure 7. SEM Pictures at high magnification showing the microstructure of the sintered alumina samples studied.

The observation of the cell walls at higher magnifications (Figs. 8 and 9) revealed a well-developed microstructure, with equiaxed grains without exaggerated grain growth and a high densification degree. The materials showed that sintering had been completed to nearly full density, without intergranular porosity and only some pores trapped inside the grains formed by coalescence of smaller grains.

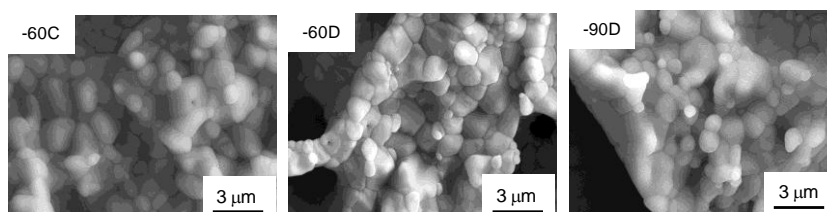


Figure 8. SEM Pictures showing the microstructure of the cross-section of the cell walls for sintered alumina samples prepared at the different cooling conditions.

Another point raised elsewhere<sup>9,18</sup> is the problem related to internal differences in the microstructure of freeze-dried compacts. As reported, irregular heat transfer causes changes in the microstructural features along the sample height, because of the temperature gradients leading to morphological differences in the orientation of the porosity channels formed during ice sublimation. To confirm this



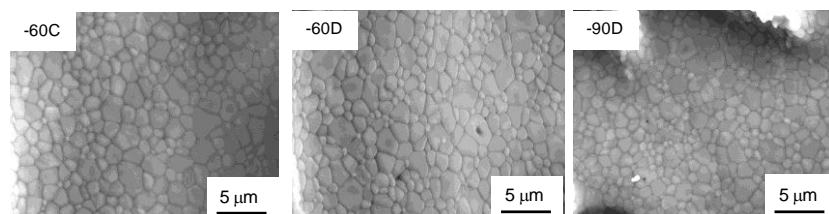


Figure 9. SEM Microstructures of the sintered alumina samples prepared at the different cooling conditions.

aspect, samples were transversally cut to obtain samples from different position along the sample height. The results were similar for all three samples, but sample –60D was selected as a case study. The samples have three regions with different density and porosity, *i.e.*, the sample bottom, in contact with the cooling metallic surface, the central body and top surface, which is the region in contact with air and at the opposite extreme of the cooling surface. Characteristic microstructures of these three regions are shown in Fig. 10. The microstructure at the sample bottom shows randomly distributed pores due to the fast freezing occurring in the vicinity to contact. The central body, which represents the major vo-

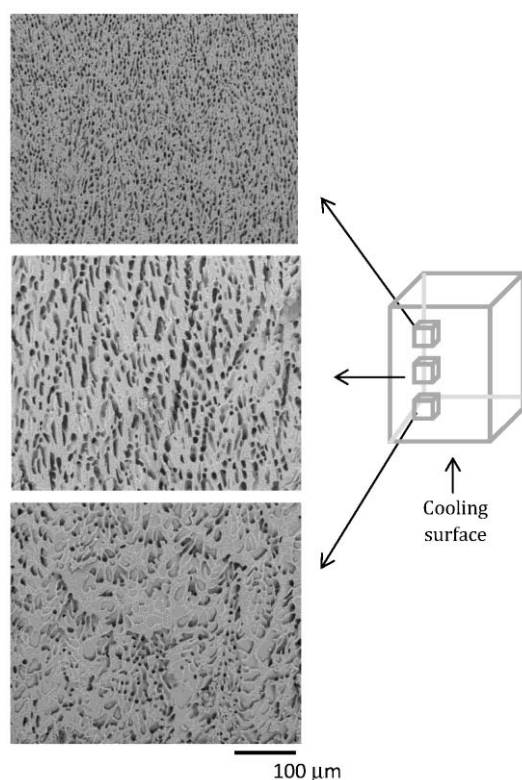


Figure 10. Characteristic SEM microstructures at different heights of freeze cast sintered specimens.

lume of the specimen, showed a higher directionality of the pores and higher uniformity at a macroscopic level. Finally, at the top of the sample, the pore alignment was lower and the size of the pores tended to decrease with respect to those observed in the body.

Summarizing the above results, it could be concluded that the main processing parameter influencing the microstructure is the cooling rate, whereas the temperature itself seems to have a negligible effect if the whole volume of the sample was frozen. Thus, by regulating the cooling rate to a constant value, it would be possible not only to shape materials with aligned porosity, but also to tailor materials with graded porosity in size and alignment.

#### CONCLUSIONS

Sintered alumina parts with aligned pores were obtained by directional freeze casting. Aqueous alumina suspensions were prepared to solids loadings of 35 vol. % and 20 wt. % of glycerol as a cryoprotector. The suspensions retained stability for at least one week. Control of cooling rate was achieved by an appropriate design of a metal support using either a metal container or a Dewar vessel to obtain different cooling rates. After sintering at 1500 °C, materials with aligned porosity and total volume of pores higher than 40 % were obtained. It was concluded that the cooling rate has a strong influence on the porosity and the microstructure, whereas temperature itself seems to have very low influence.

*Acknowledgement.* This work was supported by Spanish Ministry of Economy and Competitiveness (MAT2009-14369-C02-01).

#### ИЗВОД

#### УТИЦАЈ ТЕМПЕРАТУРЕ ХЛАЂЕЊА НА МИКРОСТРУКТУРУ И ПОРОЗНОСТ ГЛИНИЦЕ ДОБИЈЕНЕ МЕТОДОМ ЛИВЕЊА НА НИСКИМ ТЕМПЕРАТУРАМА

JESÚS M. RODRÍGUEZ-PARRA, RODRIGO MORENO и MARÍA ISABEL NIETO

*Institute of Ceramics and Glass, CSIC, Kelsen 5, 28049 Madrid, Spain*

Ливење на ниским температурама је добро позната техника обликовања приликом процесирања материјала са контролисаном порозношћу. Један од основних проблема представља контролисање брзине хлађења која проузрокује градијенте величине пора и хомогености. Тема ове студије је процесирање контролисано порозне керамике на бази глинице, полазећи од водених суспензија помоћу технике ливења на ниским температурама. Током експеримента су коришћене различите брзине хлађења. Ливење на ниским температурама је коришћена након оптимизације реолошких својстава водених суспензија глинице. Порозност и микроструктурна својства синтерованих узорака добијених под различитим условима су затим анализирана и проучавана. Закључено је да брзина хлађења у већој мери утиче на микроструктуру од коначне температуре. Микроструктурном анализом је такође показано да је постигнута контрола градијента порозности, у мањој мери при врху и на дну, а у већој мери у централном делу узорака.

(Примљено 18. новембра, ревидирано 3. децембра 2012)

## REFERENCES

1. P. Colombo, H. P. Degischer. *Mater. Sci. Technol.* **26** (2010) 1145
2. A. Corma. *Chem. Rev.* **97** (1997) 2373
3. C. Galassi. *J. Eur. Ceram. Soc.* **26** (2006) 2951
4. X. Y. Yang, Y. Li, A. Lemaire, J. G. Yu, B. L. Su. *Pure Appl. Chem.* **81** (2009) 2265
5. T. Ohji, M. Fukushima. *Int. Mater. Rev.* **57** (2012) 115
6. T. Fukasawa, Z. Y. Deng, M. Ando, *J. Am. Ceram. Soc.* **85** (2002) 2151
7. S. W. Sofie. *J. Am. Ceram. Soc.* **90** (2007) 2024
8. S. Deville. *Adv. Eng. Mater.* **10** (2008) 155
9. Y. Chino, D. C. Dunand. *Acta Mater.* **56** (2010) 105
10. K. Lu. *J. Am. Ceram. Soc.* **90** (2007) 3753
11. J. Zou, Y. Zhang, R. Li. *Int. J. Appl. Ceram. Technol.* **8** (2011) 482
12. C. Pekor, B. Groth, I. Nettleship. *J. Am. Ceram. Soc.* **93** (2010) 115
13. L. Qian, H. Zhang. *J. Chem. Technol. Biotechnol.* **86** (2011) 172
14. K. Araki, J. W. Halloran. *J. Am. Ceram. Soc.* **88** (2005) 1108
15. B. H. Yoon, Y. H. Koh, C. S. Park, H. E. Kim. *J. Am. Ceram. Soc.* **90** (2007) 1744
16. D. Koch, L. Andersen, T. Schmedders, G. Grathwohl. *J. Sol-Gel Sci. Technol.* **26** (2003) 149
17. E. Munch, E. Saiz, P. Tomsia, S. Deville. *J. Am. Ceram. Soc.* **92** (2009) 1534
18. S. Deville, E. Saiz, P. Tomsia. *Acta Mater.* **55** (2007) 1965
19. C. Tallon, R. Moreno, M. I. Nieto. *Adv. Appl. Ceram.* **108** (2009) 307
20. L. Qian, A. Ahmed, A. Foster, S. P. Rannard, A. I. Cooper, H. Zhang. *J. Mater. Chem.* **19** (2009) 5212
21. W. Li, K. Lu, J. Y. Walz. *J. Am. Ceram. Soc.* **94** (2011) 1256
22. L. Ren, Y. P. Zeng, D. Jiang. *J. Am. Ceram. Soc.* **90** (2007) 3001
23. J. W. Moon, H. J. Hwang, M. Awano, K. Maeda. *Mater. Lett.* **57** (2003) 1428
24. K. H. Zuo, Y. P. Zeng, D. Jiang. *Int. J. Appl. Ceram. Technol.* **5** (2008) 198
25. S. W. Sofie, F. Dogan. *J. Am. Ceram. Soc.* **84** (2001) 1459
26. M. N. Rahaman, Q. Fu. *J. Am. Ceram. Soc.* **91** (2008) 4137
27. C. A. Gutierrez, R. Moreno. *J. Mater. Sci.* **35** (2000) 5867.